2020

Hydrodynamic cavitation for scalable exfoliation of few layered graphene nanosheets

Steven Hiran De Alwis
Iowa State University

Hydrodynamic cavitation for scalable exfoliation of few layered graphene nanosheets

by

Steven De Alwis

A thesis submitted to the graduate faculty

in partial fulfillment of the requirements for the degree of

MASTER OF SCIENCE

Major: Mechanical Engineering

Program of Study Committee:
Nicole Nastaran Hashemi, Major Professor
Emily Smith
Reza Montazami

The student author, whose presentation of the scholarship herein was approved by the program of study committee, is solely responsible for the content of this thesis. The Graduate College will ensure this thesis is globally accessible and will not permit alterations after a degree is conferred.

Iowa State University

Ames, Iowa

2020

DEDICATION

I humbly dedicate this thesis to my family and friends. I am grateful for being given the resources to pursue my education and for the unwavering belief you always had in me.

TABLE OF CONTENTS

Page

LIST OF FIGURES

Page

ACKNOWLEDGEMENTS

I would like to express my gratitude to my committee chair, Nicole Nastaran Hashemi, and my committee members, Dr. Reza Montazami, and Dr. Emily Smith for assisting me in my research. Additionally, I am thankful to Nicholas Hunter for his contribution to materials characterization for my project.

Furthermore, I wish to extend my appreciation to the Department of Mechanical Engineering for providing me with an excellent education and an unforgettable experience.

ABSTRACT

A simple method for scalable exfoliation of biocompatible few layered graphene (FLG) dispersions is developed using an inexpensive hydrodynamic cavitation setup. Hydrodynamic cavitation is used for the exfoliation. Unlike acoustic cavitation, the primary way of bubble collapse in hydrodynamic cavitation is caused laterally, thereby separating two adjacent flakes by a shear effect. The process utilizes a known protein, Bovine Serum Albumin (BSA), which acts as an effective exfoliation agent and provides stability by preventing restacking of the graphene layers. This is because BSA possesses both hydrophobic as well as hydrophilic sections. The hydrophobic section is absorbed on graphene, which also is hydrophobic. This assists in the formation of dispersions and potentially prevents restacking of graphene. Development of potentially scalable biocompatible methods are critical for producing cost-effective non-toxic graphene, enabling numerous possible biomedical and biological applications. A methodical study was performed to identify the effect of time in a novel hydrodynamic cavitation system for graphene exfoliation. The fabricated product was characterized using Raman spectroscopy and Transmission electron microscopy. It was found that with time the number of layers of graphene seem to decrease based on the I_{2D}/I_G ratio where at 6 hours the ratio was at 0.307 but along with that disorder in graphene seem to increase based on the I_D/I_G ratio which reached up to .33 from .25 at 4.5 hours. Based on the data in the study, evidence of a direct relationship between graphene exfoliation and cavitation is found. Therefore, the paper provides the theoretical and the computational analysis needed to create an optimized cavitation model to potentially improve graphene exfoliation using hydrodynamics.

CHAPTER 1. INTRODUCTION

1.1 Overview

Graphite is a naturally occurring form of crystalline carbon. Carbon atom which consists of 6 protons, 6 neutrons and 6 electrons consists of an electron configuration of $1s^2 2s^2 2p^2$. Since the p-shell in carbon can accommodate 6 electrons to complete its octet it shares its valence electrons with other atoms by forming covalent bonds. In the case of graphite each carbon atom forms 3 covalent sigma bonds with other carbon atoms. Graphite is the 'mother material' of graphene. As opposed to graphene oxide (GO) and reduced graphene oxide (RGO), graphene and graphite has very similar characteristics [1]. Graphite naturally occurs as a 3D structure. It is found in the π-stacked hexagonal structure of graphite with an interlayer spacing of 3.34 Å, which is the van der Waals distance for sp2-bonded carbon [2]. Graphene is the hypothetical infinite aromatic sheet of sp2-bonded carbon that is the 2-D counterpart of naturally occurring 3-D graphite [3]. Graphene a crystalline allotrope of carbon is considered a single layer graphite with a honeycomb structure possessing remarkable electrical, mechanical, and thermal properties. Graphene which is a one atom thick sheet has each carbon atom covalently bonded to three other carbon atoms with sp^2 hybridization [4]. With its unique properties graphene has a market demand in sectors of automotive, industrial, medical, energy and electronics. Conduction in Single Layered Graphene (SLG) is unique compared to other conductive material studied as SLG is 2D. As an electronic material, graphene represents a new playing field for electrons in 2, 1, and 0 dimensions where its conductivity is determined using linear band structures. Band structures which correspond to the dispersion of bonding and antibonding molecular orbital are called π and π^* bands. In this thesis, the focus would be to introduce an inexpensive process to exfoliate Few Layered Graphene (FLG)

for medical applications. Graphene and its derivatives possess outstanding mechanical, electronic, optical, thermal, and chemical properties [5] Graphene could be used in the medical fields of tissue engineering, drug delivery and gene delivery [6].

1. **Tissue Engineering**

   Tissue engineering is a multidisciplinary field focused on the application of engineering and biological sciences to create a biological substitute that can repair and improve tissue's function [7]. Graphene-based materials possess mechanical properties such as high elasticity, flexibility, and adaptability to flat or irregular surfaces that are suitable for the structural reinforcement of materials frequently used for tissue engineering [8].

2. **Drug Delivery**

   Nanographene prepared at low cost with specific surface properties enables to interact with various molecules, which allow then to be used in drug delivery. These nanocarriers have primarily been used for cancer treatment to improve effectiveness and reduce side-effects [6]. For instance GO and the anticancer drug hypocrellin A complex can induce the generation of singlet oxygen molecules which can kill the impregnated cells after exposed to light irradiation [9].

3. **Gene Delivery**

   Graphene nanosheets with large sp2 hybridized carbon area, are able to interact not only with drugs, but also with other molecules like the nucleic acids DNA and RNA. Therefore, they can be used for gene delivery or as carriers and protectors of probes involved in identifying miRNAs [6]. Also, graphene is an option to deliver plasmids, especially when

functionalized with cationic polyethylenimine that interacts well with DNA's phosphate groups [10].

Graphene has a multitude of unique properties:

1. **High Electron Mobility**

Graphene possesses a band structure that is symmetric in nature, leading to elevated electron mobility [11], [12]. Scientists believe that SLG has a resistivity in the range of 10-6 ohm-cm [13].

2. **High Thermal Conductivity**

SLG has a diffusive conduction at high temperatures and a ballistic conduction at low temperatures due to its relatively low carrier density [14]. At room temperature, the monolayer graphene has a thermal conductivity of about 6000 $Wm^{-1}K^{-1}$ [15].

3. **Substantial Surface Area**

SLG has surface area equaling 2630 m^2g^{-1}. This is because its atoms are connected 2 dimensionally, causing it to have a specific surface that is larger than most materials [16], [13].

Graphene is exfoliated using multiple processes depending on its applications:

1. **Mechanochemical Exfoliation**

Earliest technique developed to exfoliate graphene was by using a scotch tape to apply normal forces on the graphene layers and its eventual acid dissolution leading to the isolation of SLG [17]. The proposed experiment setup in this thesis is an example of a mechanochemical exfoliation method.

2. Liquid Phase Exfoliation

This technique involves using surface-active organic fluids that penetrate between the layers of crystalline graphite. As a result, the increased distance between the graphene layers reduces their corresponding interaction energy. This assists in exfoliation once a mechanical force is applied on them [18].

3. Graphite Oxide Reduction

One of the most common techniques investigated to fabricate graphene is exfoliating graphite oxide into graphene oxide (GO). The motivation behind this technique is that it is relatively easier to exfoliate graphite oxide compared to graphite. However, the hydrophilicity of the GO sheet weakens during reduction [19].

4. Chemical Vapor Deposition

Chemical Vapor Deposition (CVD) involves the use of transition metal substrates to develop graphene layers. This method is based on depositing layers of nickel of transition metals on to SiO2/Si substrates using an electron-beam evaporator. Then the samples are heated up to 1000 ℃ inside a quartz tube under an argon atmosphere and cooled down to room temperature using flowing argon. This provides an efficient method of separating graphene layers from the substrate.

1.2 Research Motivation

Despite the multitude of applications available for graphene the primary focus of this thesis is to propose a process to produce graphene for medical applications. The conventional techniques in place are usually environmentally hazardous and possess toxic effects [20], [21], [22]. Therefore, there is a need to exfoliate biocompatible graphene using an efficient and an inexpensive method. To answer this Guo et al. developed a green electrochemical technique to fabricate graphene by reducing exfoliated graphite oxide (GO) [23]. Zhu et al. and Gurunathan et al. produced graphene

by reducing exfoliated GO using glucose and triethylamine respectively [22], [24]. But as explained earlier through GO it is unable to produce pristine graphene. Yi et al. produced graphene by sonicating water and alcohol and subsequently centrifuging it [25]. This method provided the main motivation developing the process presented in this thesis, for it was identified that sonication assisted in the exfoliation process and alcohol served as the primary agent in preventing the restacking of the graphene layers.

Acoustic cavitation which is a result of sonication is the primary phenomenon in exfoliating graphene. Sonication which results in acoustic cavitation generates microbubbles and thereafter results in implosions. This microbubble generation and implosion assists in providing shear forces in exfoliating the graphene and normal forces in the fragmentation of graphene.

The following chapters describe a mechano-chemical technique to exfoliate few layered graphene nanosheets in an aqueous dispersion using hydrodynamic cavitation. The process is aided by a commonly found protein, known as Bovine Serum Albumin (BSA). This also resolves the inefficiencies in sonication which primarily uses acoustic cavitation to exfoliate.

1.3 References

1. Said N et al. Comparison on Graphite, Graphene Oxide and Reduced Graphene Oxide: Synthesis and Characterization. AIP Conference Proceedings 1892(1):150002

2. Sandip Niyogi, Elena Bekyarova, Mikhail E. Itkis, Jared L. McWilliams, Mark A. Hamon, and Robert C. Haddon Journal of the American Chemical Society 2006 128 (24), 7720-7721

3. Debye, P.; Scherrer, P. Phys. Z. 1917, 18, 291-301.

4. Puzyn, Tomasz, and Jerzy Leszczynski. Towards Efficient Designing of Safe Nanomaterials: Innovative Merge of Computational Approaches and Experimental Techniques. Cambridge, UK: RSC Publishing, 2012.

5. Chen C, Lee S, Deshpande VV et al. Graphene mechanical oscillators with tunable frequency. Nat. Nanotechnol. 8(12), 923–927 (2013)

6. Tonelli FM, Goulart VA, Gomes KN, et al. Graphene-based nanomaterials: biological and medical applications and toxicity. Nanomedicine (Lond). 2015;10(15):2423-2450.

7. Tonelli FM, Santos AK, Gomes KN et al. Carbon nanotube interaction with extracellular matrix proteins producing scaffolds for tissue engineering. Int. J. Nanomedicine 7, 4511–4529 (2012).

8. Nayak TR, Andersen H, Makam VS et al. Graphene for controlled and accelerated osteogenic differentiation of human mesenchymal stem cells. ACS Nano 5(6), 4670–4678 (2011).

9. Zhou L, Wang W, Tang J, Zhou J-H, Jiang H-J, Shen J. Graphene oxide noncovalent photosensitizer and its anticancer activity in vitro. Chemistry 17(43), 12084–12091 (2011)

10. Zhang Y, Nayak TR, Hong H, Cai W. Graphene: a versatile nanoplatform for biomedical applications. Nanoscale 4(13), 3833–3842 (2012).

11.J. A. Del Alamo, Nature, 2011, 479, 317

12. E. H. Hwang and S. D. Sarma, Phys. Rev. B, 2008, 77, 115449

13. Xinran Wang and Yi Shi, CHAPTER 1: Fabrication Techniques of Graphene

14. Choongho Yu, Li Shi, Zhen Yao, Deyu Li and, Arunava Majumdar. Thermal Conductance and Thermopower of an Individual Single-Wall Carbon Nanotube. 2005 [cited 2019 Aug 5]; Available from: https://pubs.acs.org/doi/abs/10.1021/nl051044e

15.Berber S, Kwon Y-K, Tománek D. Unusually High Thermal Conductivity of Carbon Nanotubes. Phys Rev Lett [Internet]. 2000 May 15 [cited 2019 Aug 5];84(20):4613– 6. Available from: https://link.aps.org/doi/10.1103/PhysRevLett.84.4613

16.F. Schedin, A. K. Geim, S. V. Morozov, E. W. Hill, P. Blake, M. I. Katsnelson and K. S. Novoselov, Detection of Individual Gas Molecules Adsorbed on Graphene, Nat. Mater., 2007, 6, 652

17. Novoselov K S et al., Electric Field Effect in Atomically Thin Carbon Films, Science 306 666 (2004)

18. Dresselhaus M S, Dresselhaus G Adv. Phys. 30 139 (1981)

19. S. Pei and H.-M. Cheng, The reduction of graphene oxide, Carbon, 2012, 50, 3210–3228

20. S. Barwich, U. Khan and J. N. Coleman, A technique to pretreat graphite which allows the rapid dispersion of defectfree graphene in solvents at high concentration, J. Phys. Chem. C, 2013, 117, 19212–19218.

21. S. Gambhir, E. Murray, S. Sayyar, G. G. Wallace and D. L. Officer, Anhydrous organic dispersions of highly reduced chemically converted graphene, Carbon, 2014, 76, 368–377

22. Zhu, Chengzhou, et al. "Reducing sugar: new functional molecules for the green synthesis of graphene nanosheets." ACS nano 4.4 (2010): 2429-2437.

23. Guo, Hui-Lin, et al. "A green approach to the synthesis of graphene nanosheets." ACS nano 3.9 (2009): 2653-2659.

24. Gurunathan, Sangiliyandi, et al. "Microbial reduction of graphene oxide by Escherichia coli: a green chemistry approach." Colloids and Surfaces B: Biointerfaces 102 (2013): 772-777.

25. Yi, Min, et al. "A mixed-solvent strategy for facile and green preparation of graphene by liquid-phase exfoliation of graphite." Journal of Nanoparticle Research 14.8 (2012): 1003.

CHAPTER 2. HYDRODYNAMIC CAVITATION FOR SCALABLE EXFOLIATION OF FEW LAYERED GRAPHENE NANOSHEETS

Modified from a manuscript to be submitted to Ultrasonics - Sonochemistry

Steven De Alwis[1], Sarabjit Singh[1], Nicole N. Hashemi[1,2*]

[1] Department of Mechanical Engineering, Iowa State University, Ames, IA, 50010, United States of America

[2] Department of Biomedical Engineering, Iowa State University, Ames, IA, 50010, United States of America

* Email: nastaran@iastate.edu

2.1 Abstract

A simple method for protein assisted scalable exfoliation of biocompatible few layered graphene (FLG) nano-sheets is developed using hydrodynamic cavitation. Hydrodynamic cavitation is used for the exfoliation. Unlike acoustic cavitation, the primary way of bubble collapse in hydrodynamic cavitation is caused laterally, thereby separating two adjacent flakes by a shear effect. The process utilizes a known protein, Bovine Serum Albumin (BSA), which acts as an effective exfoliation agent and provides stability by preventing restacking of the graphene layers. Development of potentially scalable biocompatible methods are critical for producing cost-effective non-toxic graphene, enabling numerous possible biomedical and biological applications. A methodical study was performed to identify the effect of time in a novel hydrodynamic cavitation system for graphene exfoliation. The fabricated product was characterized using Raman spectroscopy and Transmission electron microscopy. It was found

that with time the number of layers of graphene seem to decrease based on the I_{2D}/I_G ratio where at 6 hours the ratio was at 0.307 but along with that disorder in graphene seem to increase based on the I_D/I_G ratio which reached up to .33 from .25 at 4.5 hours. The paper also provides the theoretical and the computational analysis needed to create an optimized cavitation model to potentially improve the graphene yield and fabricate higher quality graphene.

2.2 Introduction

Graphene nanosheets consists of single-, bi- or, a few, but fewer than ten, sp^2- hybridized layers of carbon atoms that are in the form of six membered rings [1]. It has a large theoretical specific surface area of 2630 $m^2\ g^{-1}$ intrinsic mobility of 200,000 $cm^2v^{-1}s^{-1}$, and a thermal conductivity of 5000 $Wm^{-1}K^{-1}$ [2-4]. Being an excellent conductor [5], it has many real-world applications and provides an ideal base for bioelectronics and biosensing. For diseases such as Parkinson's disease, understanding problems such as neurotoxicity, oxidative stress, histone deacetylase (HDAC), and other molecular pathways could be beneficial [6-7]. Graphene is helpful in understanding neurodegenerative diseases by serving as a useful biosensor, especially in understanding the electrophysiological effects on cells [8-10]. Biocompatible graphene could also be used as humidity sensors to monitor body sweat [11].

Many methods have been developed to fabricate graphene. The prominent methods can be classified as micromechanical exfoliation, electrochemical exfoliation, and exfoliation using solvents and chemical vapor deposition. Although monolayer graphene is difficult to develop, it has been observed that FLG possesses certain properties that are like monolayer graphene, such as its high surface area and the absence of gap in its electronic band structure. Due to these

similarities, FLGs can substitute for single layer graphene in various applications, ultimately generating cost effective solutions [12-16].

Lately, the influence of biological materials as exfoliates have also been investigated. Ahadian *et al.* developed graphene dispersions by sonicating graphite in Bovine Serum Albumin (BSA) media [17]. Bovine Serum Albumin is a protein that is obtained from cows through natural means. BSA possesses both hydrophobic and hydrophilic sections where the hydrophobic section is adsorbed on graphene. This assists in the formation of dispersions and potentially prevents the restacking of graphene [18].

Ultrasonication which is a process that applies sound energy to agitate particles in a sample with frequencies greater than 20kHz [19] is widely used to exfoliate graphene. It has also been proved that by optimizing acoustic cavitation (as an effect of sonication), it provides higher yields (up to 18%) of graphene [20]. Though there has been considerable research done on the topic of effects of acoustic cavitation on graphene exfoliation, an absence relating to the effects of hydrodynamic cavitation on graphene exfoliation persists. Studies comparing the effectiveness of acoustic and hydrodynamic cavitation in combined treatments found that hydrodynamic cavitation was more energy efficient as compared to acoustic cavitation [21], an essential component in the formulation of an inexpensive exfoliation method. The superior energy efficiency in hydrodynamic cavitation could provide a passage to resolve a shortcoming of acoustic cavitation; the excessive local heat generation which makes it highly restrictive for industrial applications.

Cavitation is the appearance of vapor bubbles and pockets inside an initially homogeneous liquid medium which is the breaking of a liquid medium under excessive stress. Hydrodynamic cavitation is dependent on two types of flows: flows in venturis or narrow passages (valves for

hydraulic control) and flows near the upper side of a wing or a propeller blade [22]. In this thesis Graphene exfoliation was studied based on two main patterns of vapor cavities namely cavitating vortices (CV) using a kitchen blender and transient isolated bubbles (TIB) using the novel experimental model.

Raman spectroscopy is widely used for structural characterization of new carbon-based materials [23]. Therefore, using Raman spectroscopy, the graphitic nature of the samples produced through the blender and the novel experimental model could be compared. Sequentially, the systematic effect of time on graphene exfoliation would be studied using the proposed cavitation model.

2.3 Materials and Method

Bovine Serum Albumin (BSA) (CAS: 9048-46-8) and Graphite (powder, <20 μm, synthetic, CAS: 7782-42-5) were purchased from Sigma Aldrich USA for the graphite solution. As for the solvent, deionized water was used.

2.4 Results and Discussion

2.4.1 Effect of cavitating vortices in graphene exfoliation

Initially to identify the bubble propagation on the blades of the blender a high-speed image of the bubbles created on the tip of the blades were taken to prove the existence of cavitation. For visibility reasons the images were taken in the presence of water instead of the graphite solution. Thereafter, the graphite solution was introduced to the blender and was run for 30 minutes at a medium speed (Figure 1). The concentration of graphite was kept constant at 20g in each

experiment throughout the study. The concentration of BSA was kept constant at 610 mg. In addition, 600 mL of water was added to the graphite-BSA mixture to prepare a solution. The experimental set up is like the setup developed by Pattammattel et al [24].

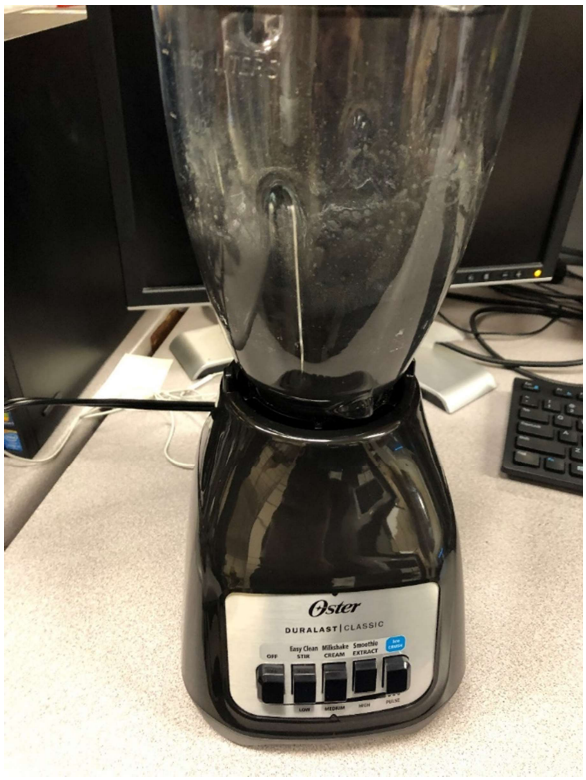

Figure 2.1 Graphene exfoliation using a kitchen blender

2.4.2 Effect of transient isolated bubbles in graphene exfoliation

The proposed model (Figure 2) consisted of a centrifugal pump which is rated at a maximum pressure of 10 psi, and a flow rate of 11 GPM. As for the point of cavitation, a needle valve with a flow coefficient of 0.87 was used. Since this was a centrifugal pump, flow was inconsistent throughout the experiment as flowrate varies with respect to output pressure. This could be considered a significant drawback in this experimental model because having a constant flow is ideal for studying cavitation. The orifice created in the needle valve served as being the venturi or the constriction in this setup. The constriction assists in increasing the velocity of the fluid

thereby decreasing the cavitation number. The cavitation number is an important factor because cavitation occurs at lower range.

As for the graphite solution introduced to the model the concentration of graphite was kept constant at 30 g in each experiment throughout the study. The concentration of BSA was kept constant at 910 mg, and 900 mL of water was added to the graphite-BSA mixture to prepare the solution. The graphite solution introduced to the proposed model was initially mixed in the blender for 5 minutes under a low speed, after which the dynamic viscosity and the specific gravity was measured. Afterwards, the kinematic viscosity was calculated using both measured values.

Figure 2.2 Graphene exfoliation using the cavitation setup with a needle valve

2.4.3 Material properties of the graphite solution

Viscosity is the transport property of the fluids that serves as quantitative data to design mass transfer, heat transfer and fluid flow mechanism [25]. By measuring the time for a volume of liquid to flow under gravity, the dynamic viscosity can be obtained by multiplying the kinematic viscosity by the density of the fluid [26]. Density of the fluid (ρ_{GS}) was found as a product of the measured specific gravity of the graphite solution (SG_{GS}) and density of water (ρ_{water}).

$$\rho_{GS} = SG_{GS} * \rho_{water} (1)$$

The measured dynamic viscosity of the graphite protein solution was 1.1429 cP as opposed to the dynamic viscosity of water which is 1 cP. The specific gravity of the solution is 1.0105 which results in the solution's kinematic viscosity to be 1.131 cSt. The density of the solution is 1010.5 kg/m^3 .

$$\nu_{GS} = \frac{\mu_{GS}}{\rho_{GS}} (2)$$

2.4.4 Graphene exfoliation using the kitchen blender

Raman spectroscopy was used to investigate the exfoliation of graphene. Using the ratio of peak intensities I_D/I_G, one can use Raman spectra to characterize the level of disorder in graphene. The number of layers can be derived from the ratio of peak intensities, I_{2D}/I_G, as well as the position and shape of these peaks [27]. Using the spectroscopy, it was found that the I_D/I_G was 0.5 and the I_{2D}/I_G was 0.375 (Figure 3). The spectroscopy seemed to replicate the data of experiments performed by Guo et al [28], although the I_D/I_G seemed to be higher in this instance. It could be

seen on the images taken of the blade of the blender using a high-speed camera that cavitation was the governing phenomenon in graphene exfoliation (Figure 4).

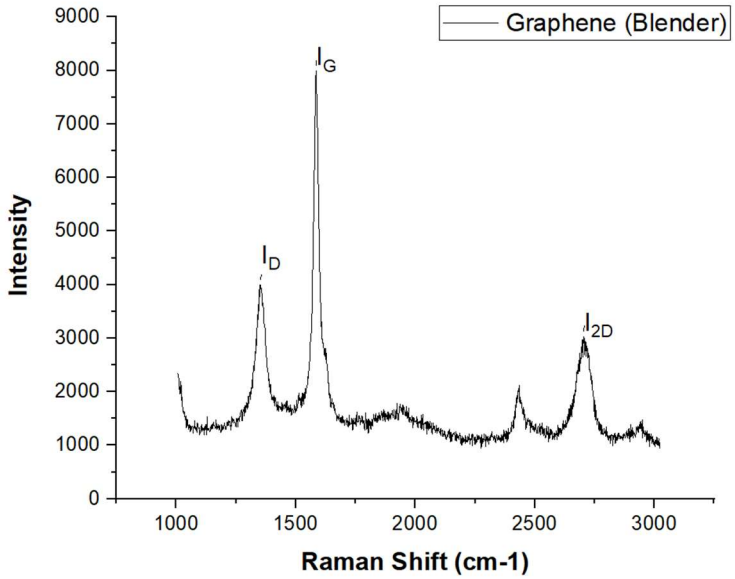

Figure 2.3 Raman spectra for the graphene exfoliated using the blender

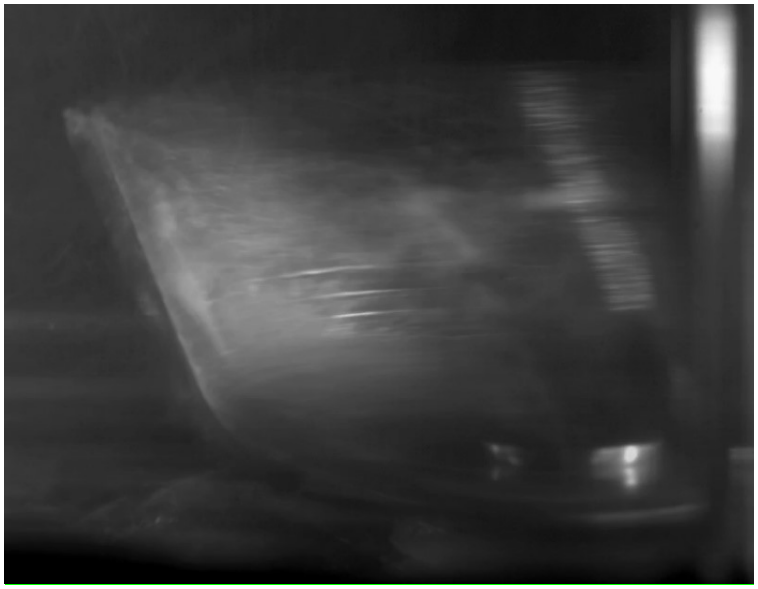

Figure 2.4 High speed image of the bubbles created due to cavitation on top of the blender blade

2.4.5 Effects of temperature in graphene exfoliation

The motivation behind this study were the findings by Abu-Rahmeh et al [29] where it was found that cavitation increases with temperature and flow rate. To understand the effects temperature on graphene exfoliation an experiment was design using the kitchen blender setup. In this experiment, temperature was assigned to be the independent variable while the Raman spectra data gathered of the graphene samples were treated to be the dependent variable. The graphite solutions were prepped in a flak before being introduced to the blender. Experimental group's solution was heated while in the flask. Both solutions of the controlled and the experimental groups were blended at a constant speed for 30 minutes. After which samples were collected.

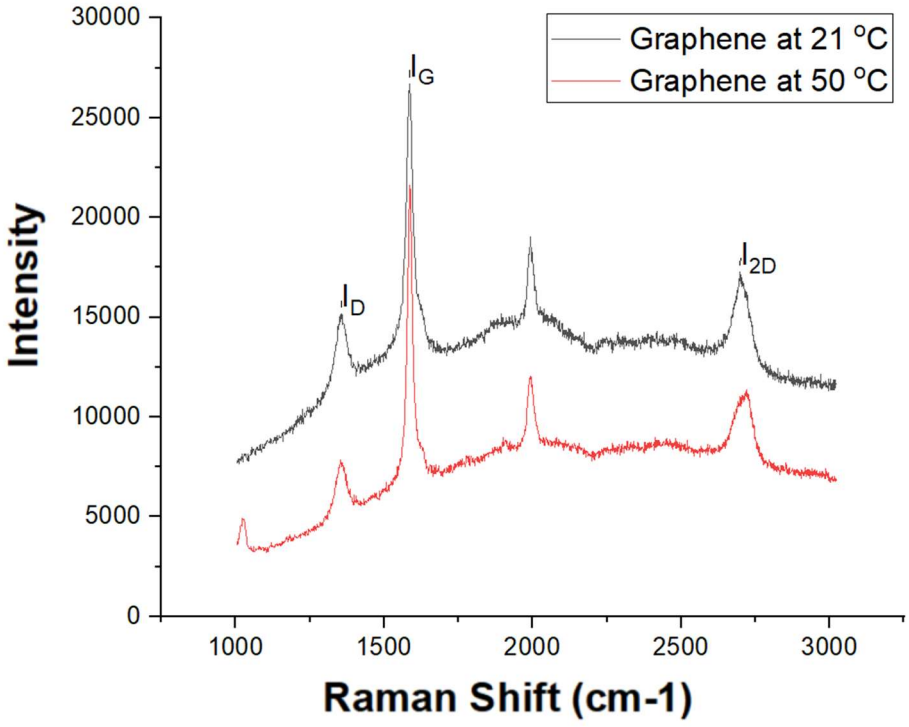

Figure 2.5 Raman spectra for the graphene exfoliated by varying temperatures

It was found using the spectroscopy of the samples that the I_{2D}/I_G ratio of graphene at 50 Celsius was .476 and at 21 Celsius (room temperature) was .648 (Figure 5). This is proof that at higher temperatures, the graphene produced tend to have a smaller number of layers.

2.4.6 Graphene exfoliation using the proposed model

Graphene exfoliation in the proposed cavitation model was studied using 3 main time intervals of 3, 4.5 and 6 hours. Similarly, both the I_D/I_G and I_{2D}/I_G ratios were calculated for each run to study the graphitic nature of the graphene produced. At 3 hours it was found the I_D/I_G to be 0.29 and I_{2D}/I_G to be 0.43. At 4.5 hours it was found the I_D/I_G to be 0.25 and I_{2D}/I_G to be 0.33. At 6 hours it was found the I_D/I_G to be 0.33 and I_{2D}/I_G to be 0.307. Based on these ratios it could be seen that though the I_D/I_G ratios did not necessarily change with time I_{2D}/I_G seem to show lower ratios with increasing time (Figure 6). These results suggest that, with time, graphene exfoliation tends to improve. To understand the morphology of the graphene produced TEM images were used. These images provided an insight to the number of layers of the graphene produced which was used in ranking the graphene. It was identified that the graphene processed for six hours tend to be less opaque (Figure 7a) meaning there were a smaller number of graphene layers than that of the other two samples (Figure 7b, Figure 7c).

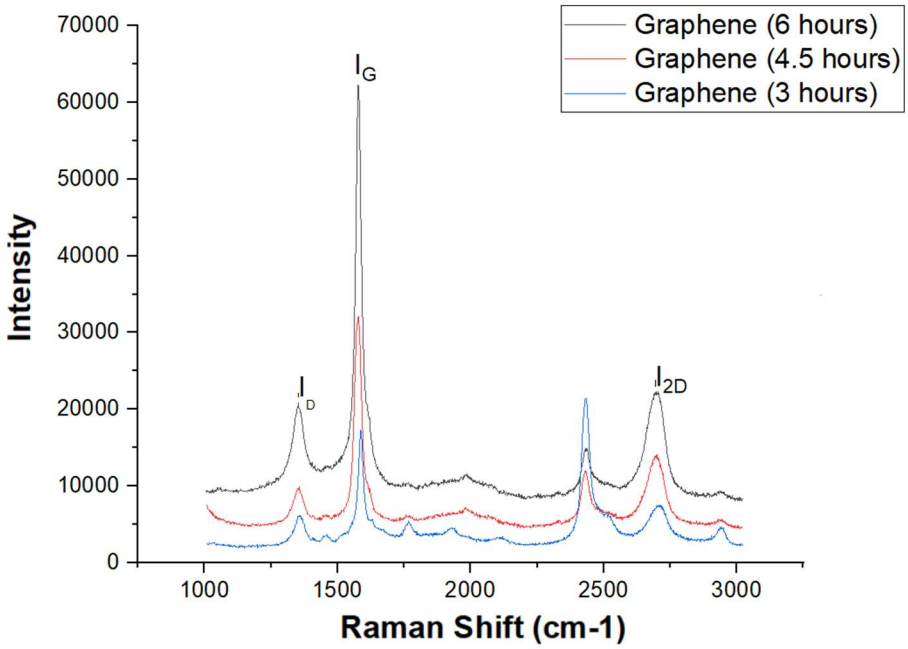

Figure 2.6 Raman spectra for the graphene exfoliates using the proposed cavitation model. Data gathered for time periods of 3 hours (Blue), 4.5 hours (Red), 6 hours (Black)

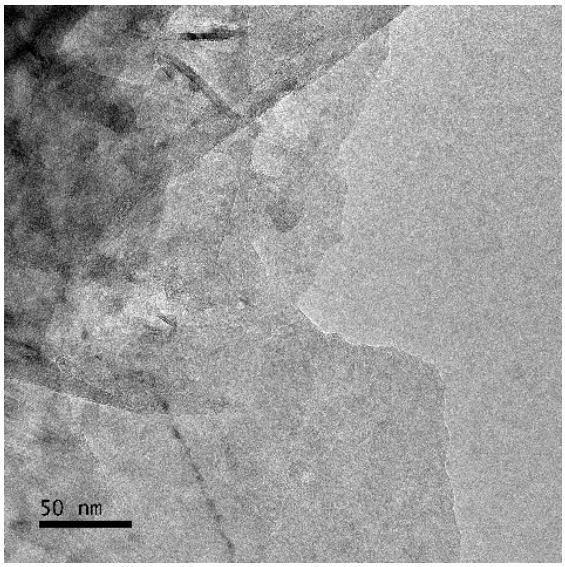

Figure 2.7 Transmission Electron Microscopy Images for graphene exfoliated using the setup with a needle valve: (a) Exfoliated for 6 hours (b) Exfoliated for 4.5 hours (c) Exfoliated for 3 hours

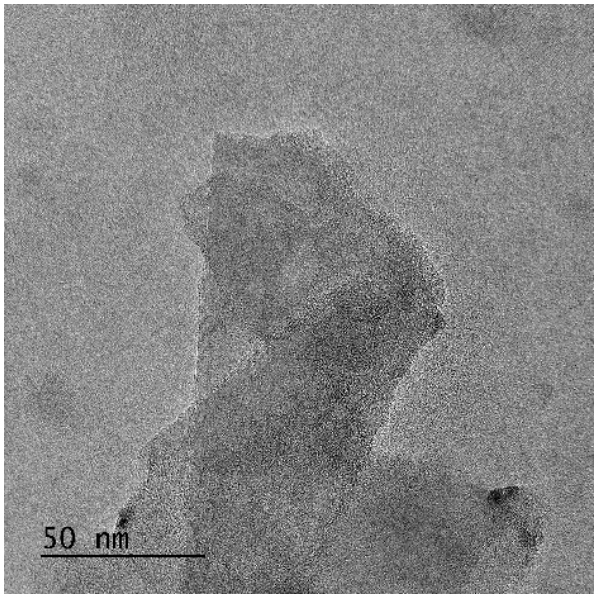

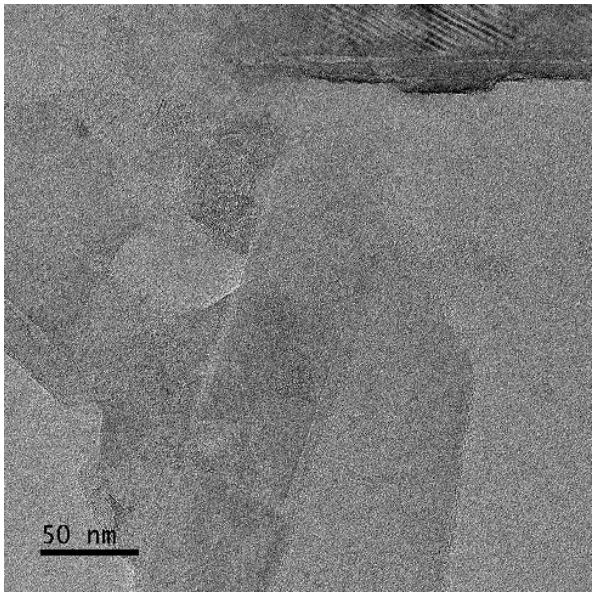

Figure 2.7 Continued

2.4.7 Optimized cavitation model using a venturi tube

Based on data gathered by Li et al [29] on cavitation a COMSOL model was created to size a potential pump and study the effectiveness of a potential venturi tube to create hydrodynamic cavitation. A venturi tube was designed using SolidWorks (Figure 8a) with a diameter ratio (DR) of 6, where in the inlet diameter (D_i) was 9mm and 1.5mm for the orifice diameter (D_0) (Figure 8b).

$$DR = \frac{D_i}{D_0} \quad (3)$$

An inlet angle of 19 degrees and an outlet angle of 5 degrees was assigned to optimize cavitation (Figure 6). This was because the highest-pressure drops were found in these angles based on findings of Li et al [30]. Using the simulation, it was seen the pressure dropped to vapor pressure at the throat of the venturi tube (Figure 9c). The cavitation number (C_v) is a dimensionless number used to characterize the conditions of cavitation in hydraulic devices. The cavitation number is dependent on P_i inlet pressure, P_v vapor pressure, density of the graphite solution and v_0 which is the solution velocity at the orifice (throat).

$$C_v = \frac{P_i - P_v}{\frac{1}{2} * \rho_{GS} * v_0} \quad (4)$$

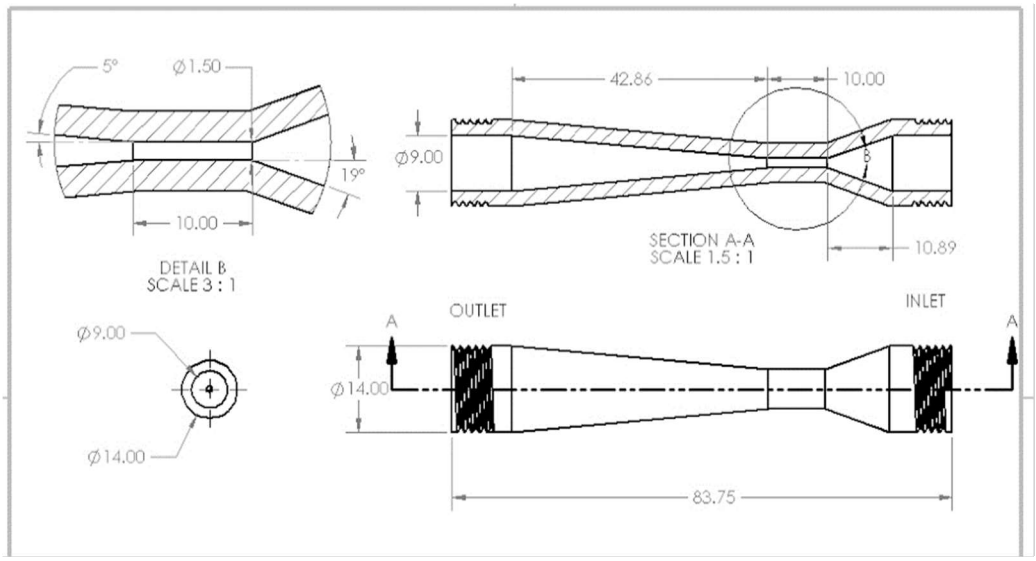

Figure 2.8 Venturi tube designed to optimize cavitation: (a) 3D model (b) 2D sketch

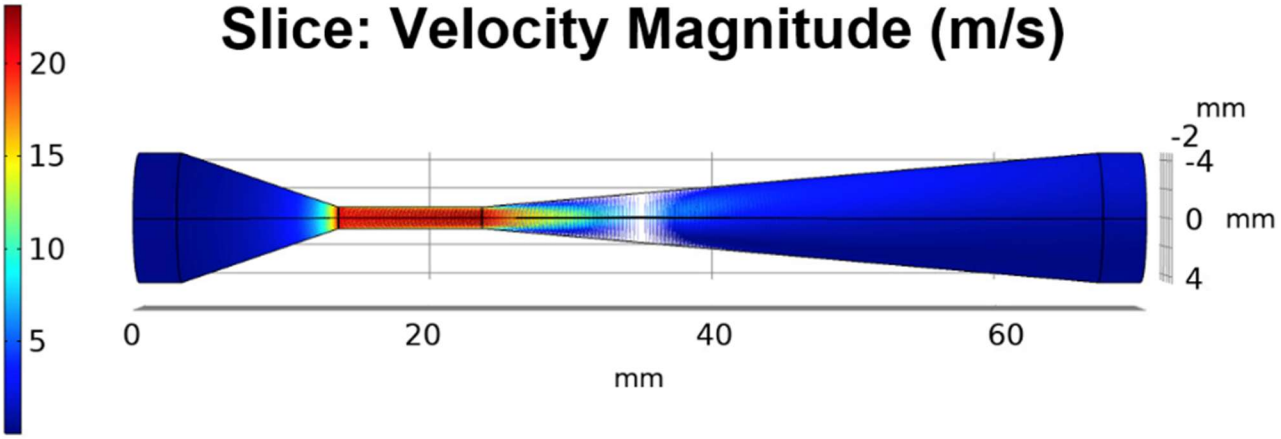

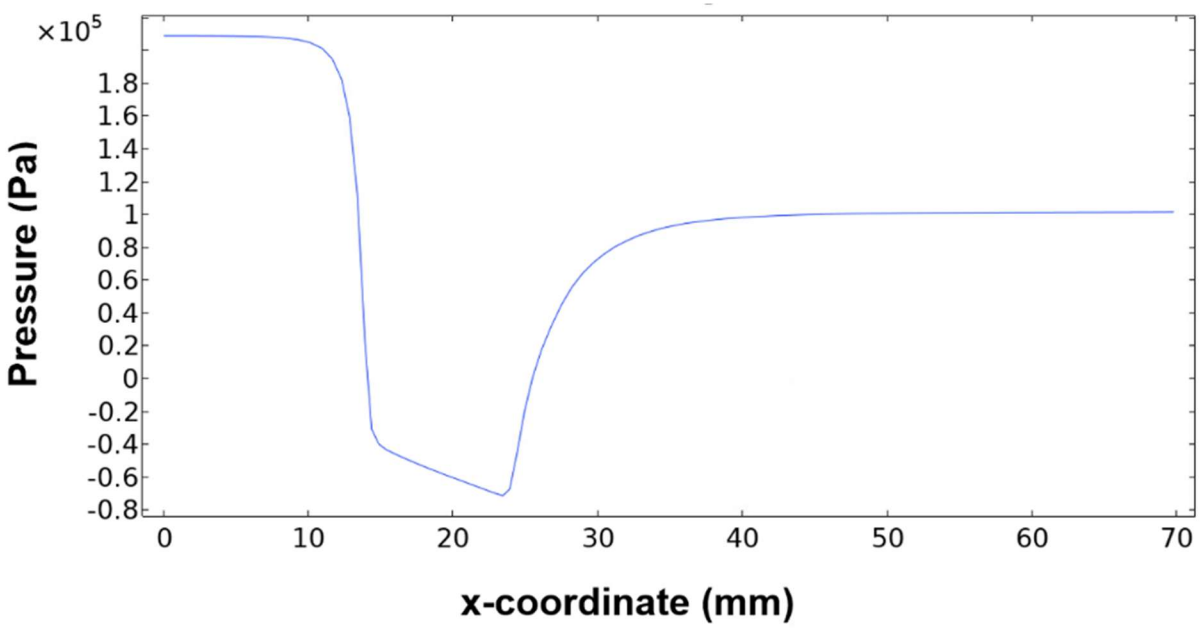

Figure 2.9 COMSOL Simulation of the venturi tube: (a) Velocity vs displacement graph (b) Pressure vs displacement graph (c) Velocity vs displacement model

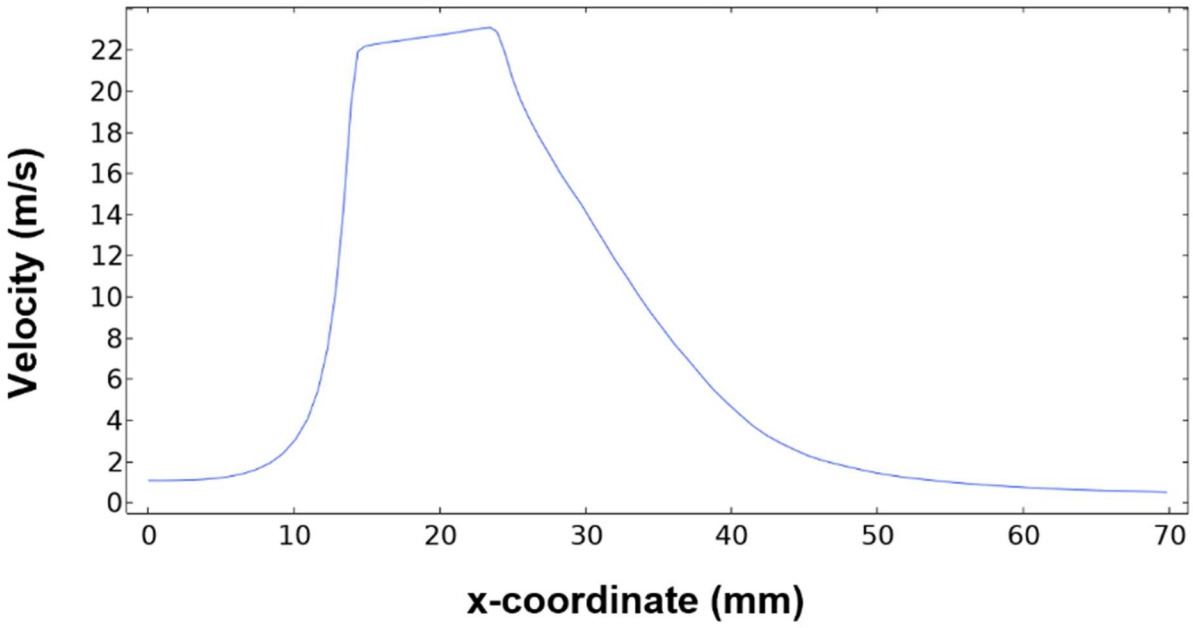

Figure 2.9 Continued

The proposed venturi tube was able to achieve a cavitation number of 0.909 with inlet pressure of 190kPa (Figure 9b) and an orifice speed of 23 m/s (Figure 9c). Using the simulation, it was also identified a pressure drop of 250kPa was achieved (Figure 9b). Based on this analysis it is recommended for future graphene exfoliation studies a positive displacement pump be utilized. If the cavitation number is needed to be improved, it is recommended findings of Vichare et al [31] be incorporated to the experimental procedure.

By potentially introducing an orifice plate as suggested in the paper by Vichare et al it would be possible to decrease the cavitation number by arranging more openings of small size on the plate by increasing the total perimeter of the holes.

Understanding flows and pressures is pivotal for this study and therefore including a pressure gauge and a flow meter would be essential in effectively gathering data (Figure 10). Unlike the

hydraulic circuit by Li et al[30] a flow damper would not be necessary in this instance, for recirculation of bubbles would be beneficial in graphene exfoliation. Due to the low pressure the complete setup would be able to be built using PVC pipes. As for the pressure gauge and pump connections, it is possible to use CPVC stainless steel female and male adapters respectively to avoid internal corrosion if process is intended to use for longer duration.

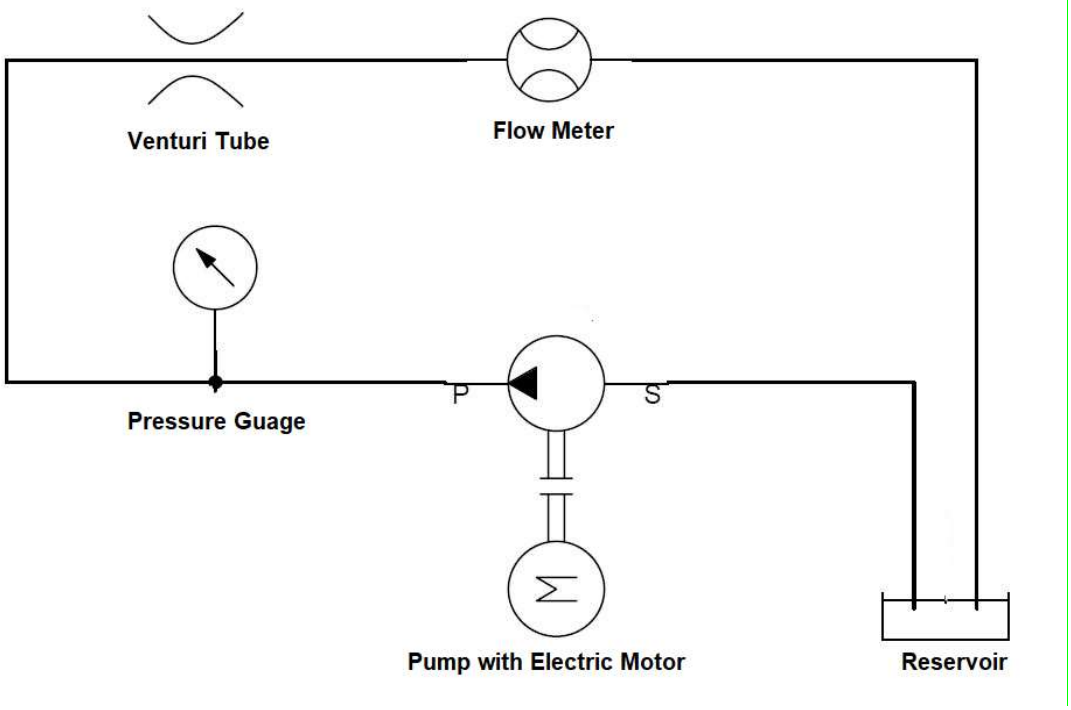

Figure 2.10 Hydraulic circuit for the optimized cavitation model for graphene exfoliation

A simulation was performed using ANSYS to understand the effects of temperature and flow rate on cavitation as prescribed by Rahmeh et al [29]. Here the designed venturi tube was subjected to a multiphase fluid flow with varying flow rates and inlet temperatures. In this study data relating to change of velocity and vapor volume fraction in the venturi tube were simulated. Identifying the vapor volume fraction helps in understanding the number of microbubbles generated for when the vapor volume concentration increases it indicates that more microbubbles are generated due to cavitation as liquid pressure drops to vapor pressure.

In this simulation data relating to two flow rates and three temperatures at a constant gauge pressure of 190 kPa (27 psi) were gathered. The two flowrates were intended to create velocities of 2 m/s and 4 m/s at the inlet of the venturi tube at temperatures of 298K, 323K and 350K.

It was found that increments in temperature seem to increase the vapor volume of the cavitated fluid (Figure 8a and Figure 8b). Increase in vapor volume also seem to depend on increments in flow rate (Figure 8c, Figure 8d and Figure 8e, Figure 8b). Yet large increments in temperatures seem to decrease throat velocity of the fluid (Figure 8f). Overall, findings through this study suggests that to optimize cavitation in a fluid it is ideal to increase both the flowrate and the temperature.

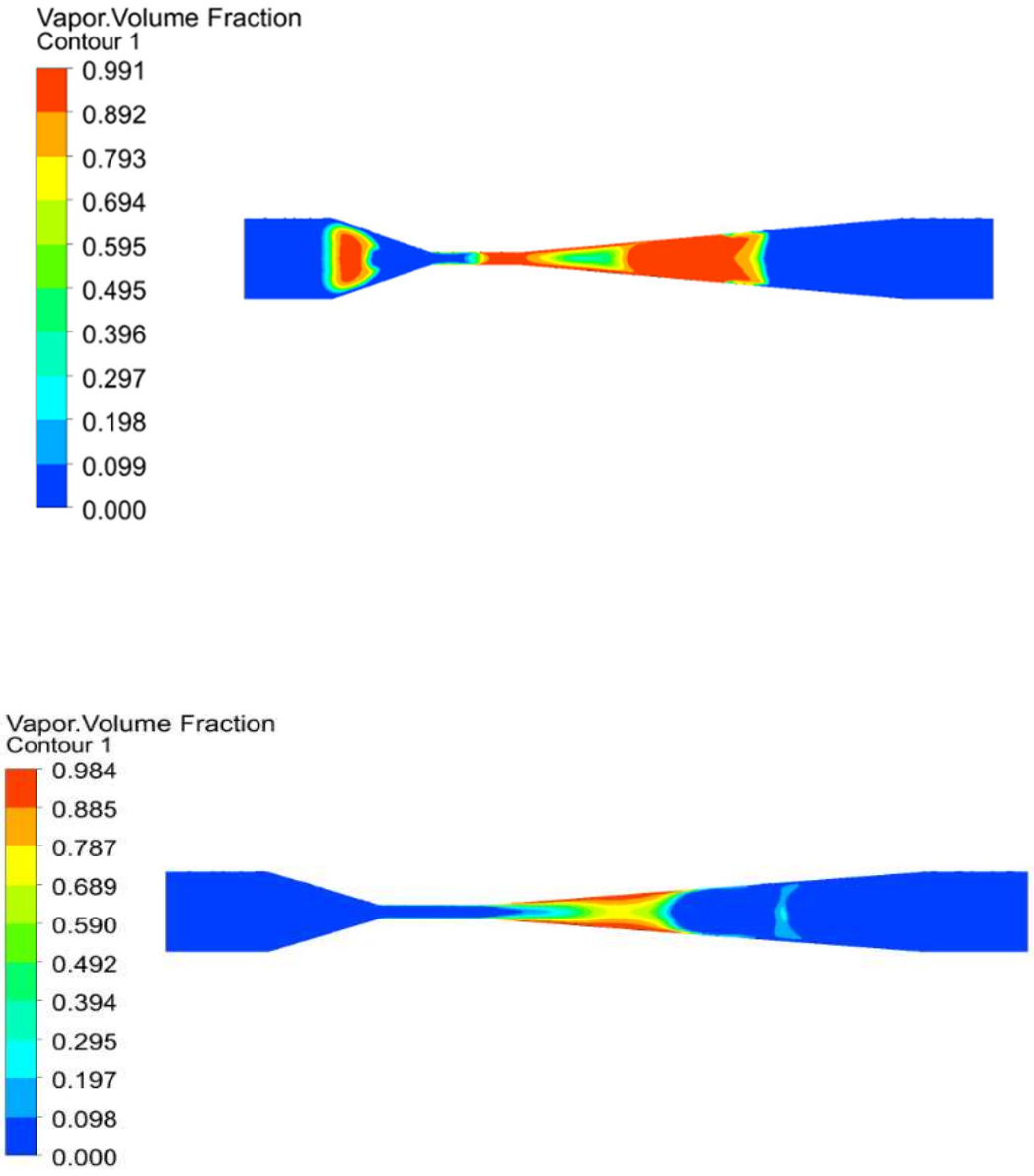

Figure 2.11. ANSYS Simulation of the venturi tube: (a) Vapor volume fraction at inlet velocity 4m/s at 350K (b) Vapor volume fraction at inlet velocity 4m/s at 298K (c) Vapor volume fraction at inlet velocity 2m/s at 323K (d) Vapor volume fraction at inlet velocity 4m/s at 323K (e) Vapor volume fraction at inlet velocity 2m/s at 298K (f) Velocity contour at inlet velocity 4m/s at 350K

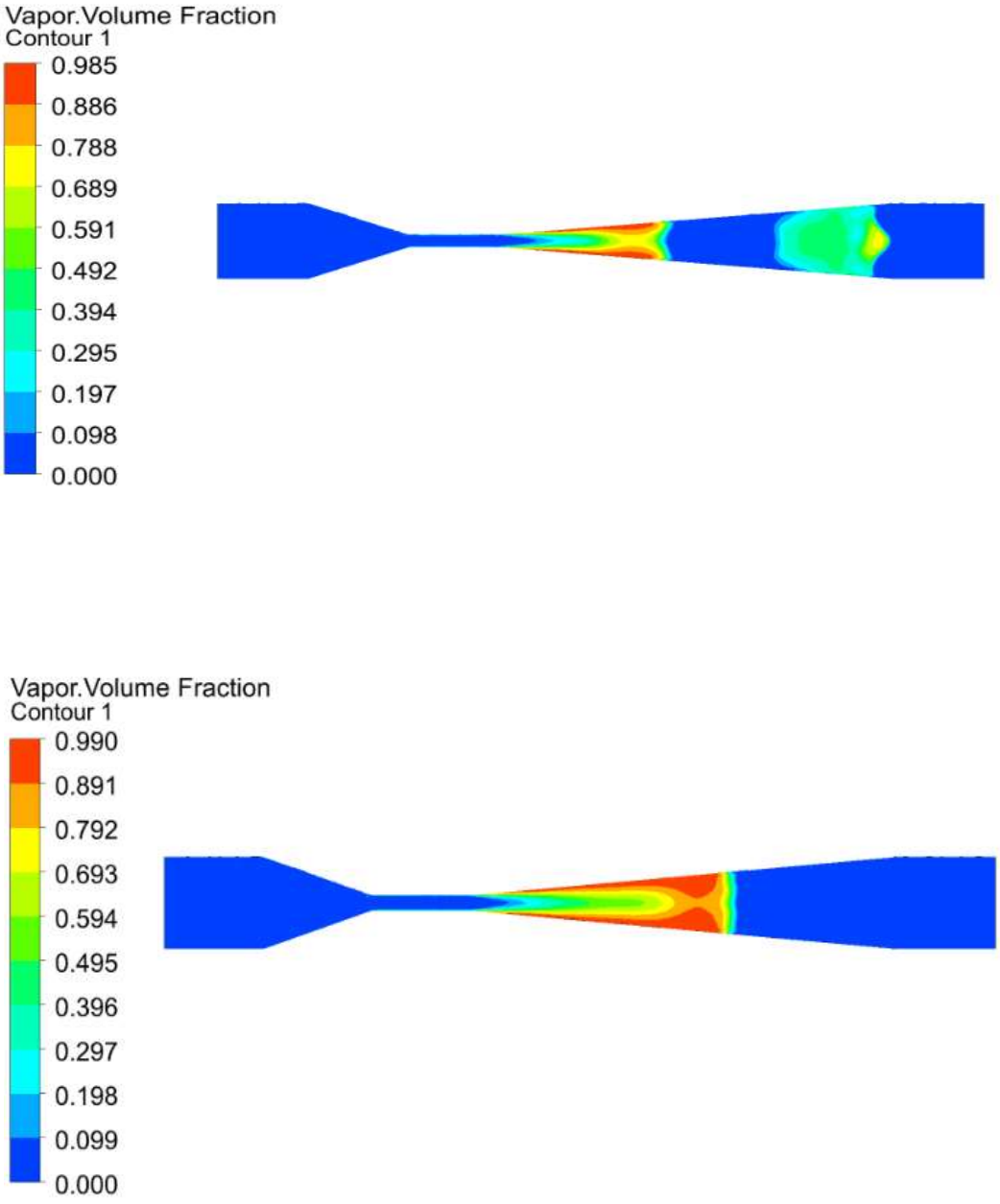

Figure 2.11 Continued

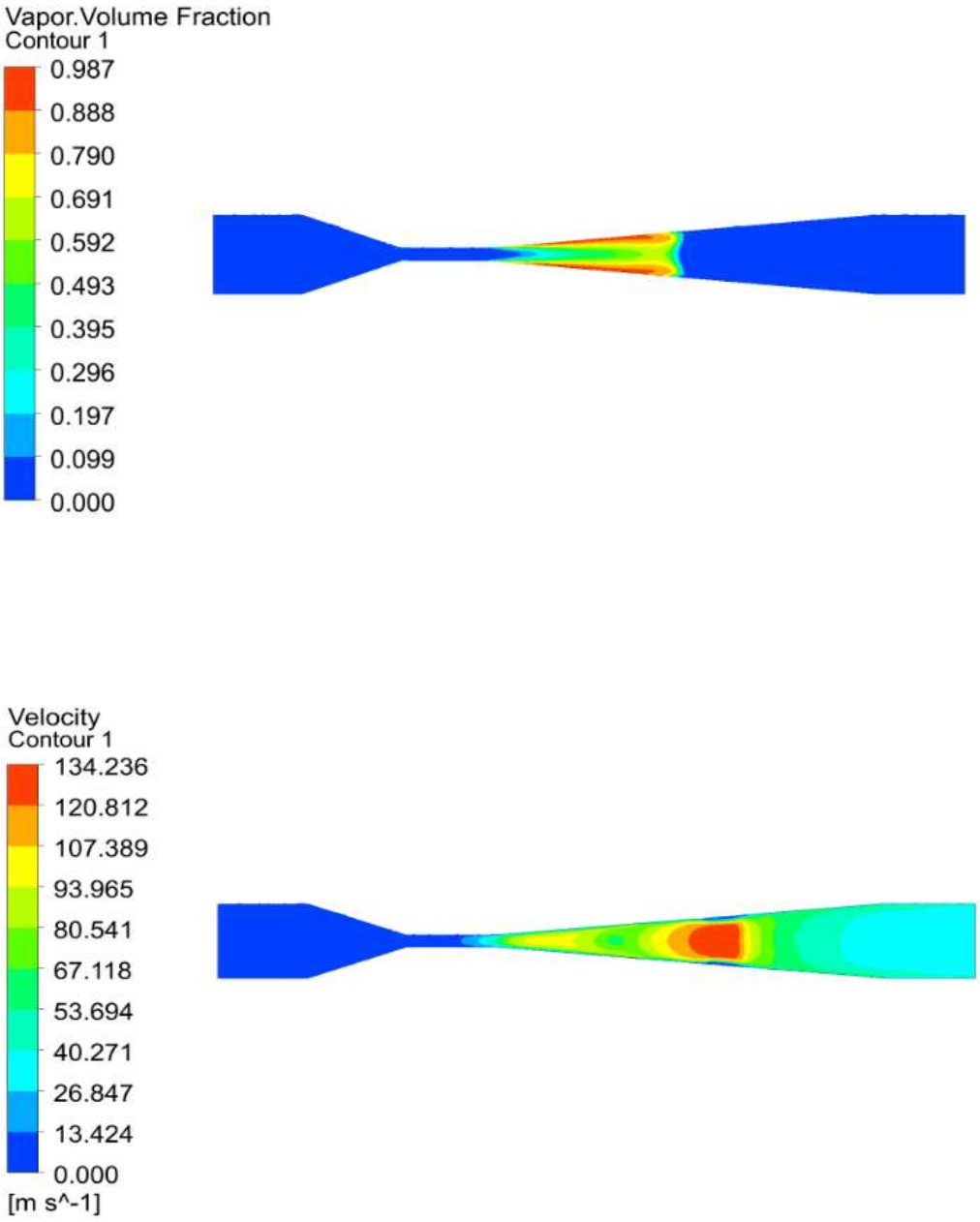

Figure 2.11 Continued

Using the optimized gauge pressure found in Figure 9b, throat velocities found using ANSYS simulations and equation 4, the respective cavitation numbers were computed.

Table 2.1. Cavitation numbers for the ANSYS simulations

T (K)	P_i (kPa)	P_v (Pa)	ρ_{GS} $(\frac{kg}{m^3})$	$v_0(\frac{m}{s})$	C_v
350	190	41.68	1010.5	136	0.0159
323	190	12.26	1010.5	161	0.0136
298	190	3.142	1010.5	161	0.0143
323	190	12.26	1010.5	81	0.0536
298	190	3.142	1010.5	81	0.0564

Based on the cavitation numbers computed it was identified the lowest cavitation number was at 323K with an inlet velocity of 4m/s. Though increase in temperature assisted in decreasing the cavitation number which is evidence for improvement in cavitation, with larger temperature increments the throat velocity seems to decrease and therefore the cavitation number was higher than that of an instance where the throat velocity was relatively higher.

2.4.8 Experimental design for optimized cavitation model using a venturi tube

Based on the experimental setup using the needle valve it was proved that hydrodynamic cavitation has a direct relationship with graphene exfoliation. Using the computational data from the ANSYS simulation it was proved that increments in both temperature and flowrate has a direct relationship in increasing hydrodynamic cavitation; with flowrate acting as a larger contributing factor at minor increments in temperature. Since it is relatively difficult to control

the temperature in a flow in the experimental model the primary focus should be to vary flow rate to understand its effect in graphene exfoliation.

For this design to supply an inlet velocity of 6 m/s at the venturi tube a pump which can supply a flow of over 6 GPM must be used. This is because the inlet diameter of the venturi is 9 mm and therefore it must see a flow of 6 GPM to produce an inlet velocity of 6 m/s. In order to experimentally study the effect of flowrate on graphene exfoliation it is recommended a prime mover which could change the speed of the pump is being used or else to include a flow adjustment valve in the circuit proposed in Figure 10.

2.5 Conclusion

In conclusion, an inexpensive method to exfoliate biocompatible graphene is presented. This paper would act as an effective introduction to the field of biocompatible graphene exfoliation using hydrodynamics. Based on the results, it could be concluded that processing time reduces the number of layers of graphene, yet the level of disorder seems to increase. As it was recorded the I_{2D}/I_G and I_D/I_G ratios to be .307 and .33 respectively at 6 hours. Based on the data of the effects of temperature on graphene exfoliation it could be identified with increase in temperature graphene exfoliation improves as the I_{2D}/I_G ratios improved accordingly. This is because with increase in temperature cavitation improves. This paper also provides adequate information to further study the effects of cavitation in graphene exfoliation. This design has proven that cavitation is the governing phenomenon in fluid based mechanochemical graphene exfoliation. This paper has provided an entrance to study graphene exfoliation based on other hydrodynamic principles.

This paper has also provided the analysis required for a potential optimized cavitation model which would assist in gathering further information relating to the impact of cavitation on graphene exfoliation by evaluating the effects of temperature and flowrate on cavitation.

2.6 Experimental

Raman spectroscopy

A thin film of the graphene sample was prepared to determine the Raman spectra. An approximately 10 mm-diameter drop of graphene sample was dropped on top of a Si/SiO2 substrate and was air-dried. The spectra were collected from 600-3300 cm^{-1}.

Transmission Electron Microscopy (TEM)

The TEM images were taken using a JEOL 2100 Scanning and Electron Microscope. The samples were placed on a silicon wafer by pipetting 2 μL of the aqueous FLG dispersions prior to it being placed within the microscope.

Acknowledgement

This work was partially supported by the Office of Naval Research Grant N000141712620. The authors would like to thank Nicholas Hunter for his contribution to materials characterization.

2.7 References

1. D. Thomas, E. Kavak, N. Hashemi, R. Montazami, N. Hashemi. Synthesis of graphene nanosheets through spontaneous sodiation process. *Journal of Carbon Research*. 2018*,* **4**, 42

2. W. Cai, Y. Zhu, X. Li, R. Piner, R. Ruoff. Large area few-layer graphene/graphite films as transparent thin conducting electrodes. *Appl Phys Lett*. 2009, **95**, 123115

3. Y. Shao, J. Wang, H. Wu, J. Liu, I. Aksay, Y. Lin. Graphene based electrochemical sensors and biosensors: A review. *Electroanalysis*. 2010, **2**,103

4. Y. Xie, P. Yuan , T. Wang, N. Hashemi, X. Wang. Switch on the high thermal conductivity of graphene paper. *Nanoscale*, 2016, **8**, 17581

5. R. Edwards, K. Coleman, Graphene synthesis: relationship to applications. *Nanoscale*. 2013, **5**, 38-51

6. L. Gao, W. Zhou, B. Symmes, C. Freed. Re-Cloning the N27 Dopamine Cell Line to Improve a Cell Culture Model of Parkinson's Disease. *PLOS One*, 2016, **11**

7. X. Che, J. Boldrey, X. Zhong, S. Unnikandam-Veettil , I. Schneider, D. Jiles. On-Chip Studies of Magnetic Stimulation Effect on Single Neural Cell Viability and Proliferation on Glass and Nanoporous Surfaces. *ACS Appl Mater Interfaces*. 2018, **10**,28269-28278

8. D. Harischandra, H. Jin, V. Anantharam, A. Kanthasamy, A. Kanthasamy. α-Synuclein Protects Against Manganese Neurotoxic Insult During the Early Stages of Exposure in a Dopaminergic Cell Model of Parkinson's Disease. *Toxicol Sci*. 2015, **143**,454-68

9. Y. Wang, X. Wang, L. Liu, X. Wang. HDAC inhibitor trichostatin A-inhibited survival of dopaminergic neuronal cells. *Neurosci Lett*. 2009, **467**, 212-216

10. A. Alsi, J. Guo, P. Lai, R. Montazami, N. Hashemi. High-Yield Production of Aqueous Graphene for Electrohydrodynamic Drop-on-Demand Printing of Biocompatible Conductive Patterns. *Biosensors*. 2020, **10**

11. J. Bao, N. Hashemi, J. Guo, N. Hashemi. Effects of graphene layer and gold nanoparticles on sensitivity of humidity sensors. *Journal of Micromanufacturing*. 2020

12. C. Berger, Z. Song, X. Li, X. Wu, N. Brown, C. Naud, D. Mayou, T. Li, J. Hass, A. Marchenkov, E. Conrad, P. First, W. de Heer. Electronic Confinement and Coherence in Patterned Epitaxial Graphene. *Science*. 2006, **5777**, 1191-1196

13. A. Geim, K. Novoselov. The rise of graphene. *Nature Materials*. 2007, **6**, 83–191

14. Y. Hernandez, V. Nicolosi, M. Lotya, M. Blighe, Z. Sun, S. De, I. McGovern, B. Holland, M. Byrne, Y. Gun'Ko, J. Boland, P. Niraj, G. Duesberg, S. Krishnamurthy, R. Goodhue, J. Hutchison, V. Scardaci, A. Ferrari, J. Coleman. High-yield production of graphene by liquid-phase exfoliation of graphite. *Nature Nanotechnology*. 2008, **3**, 563–568

15. M. Batzill. The surface science of graphene: Metal interfaces, CVD synthesis, nanoribbons, chemical modifications, and defects. *Surface Science Reports*. 2012, **67**, 3-4

16. S. Morozov, K. Novoselov, F. Schedin, D. Jiang, A. Firsov, A. Geim. Two-dimensional electron and hole gases at the surface of graphite. *Physical Review B*. 2005

17. V. González, A. Rodríguez, V. León, J. Frontiñán-Rubio, J. Fierro, M. Durán-Prado, A. Muñoz-García, M. Pavone, E. Vázquez. Sweet graphene: exfoliation of graphite and preparation of glucose-graphene cocrystals through mechanochemical treatments. *Green Chemistry*. 2018, **20**, 3581-3592

18. Safety Information - Sigma Aldrich. https://www.sigmaaldrich.com/catalog/product/sial/227056?lang=en&region=US.

19. R. Tan, S. Reeves, N. Hashemi, D. Thomas, E. Kavak, R. Montazami, N. Hashemi. Graphene as a flexible electrode: review of fabrication approaches. *Journal of Materials Chemistry A*. 2017, **2**, 37-54

20. P. Turner, M. Hodnett, R. Dorey, J. David. Controlled sonication as a Route to in-situ Graphene Flake size Control. *Nature Materials*. 2019, **9**, 8710

21. P. Gogate, G. Bhosale. Comparison of effectiveness of acoustic and hydrodynamic cavitation in combined treatment schemes for degradation of dye waters. *Chemical Engineering and Processing: Process Intensification.* 2013, **71**, 59-69

22. J.M. Michel. Introduction to Cavitation and Supercavitation; Supercavitating flows, 2001

23. C. Castiglioni, F. Negri, M. Rigolio, G. Zerbi. Raman activation in disordered graphites of the A 1′ symmetry forbidden k≠ 0 phonon: the origin of the D line. *The Journal of Chemical Physics*. 2001, **115**, 3769

24. V. León, M. Quintana, M. Herrero, J. Fierro, A. Hoz, M. Prato, E. Vázquez. Few-layer graphenes from ball-milling of graphite with melamine. *Chemical Communications*. 2011, **47**, 10936-10938

25. S. Alam, B. Ashokkumar, M. Siddiq. The density, dynamic viscosity and kinematic viscosity of protic polar solvents (pure and mixed systems) studies: A theoretical insight of thermophysical properties. *Journal of Molecular Liquids*. 2018, **251**, 458-469

26. Standard Test Method for Kinematic Viscosity of Transparent and Opaque Liquids (and the Calculation of Dynamic Viscosity). An American National Standard British Standard, 2000

27. I. Childres, L. Juaregui, W. Park, H. Cao, Y. Chen. *Raman spectroscopy of graphene and related materials* [Online]. http://citeseerx.ist.psu.edu/viewdoc/download?doi=10.1.1.708.1042&rep=rep1&type=pdf

28. J. Guo, A. Asli, K. Williams, P. Lai, X. Wang, R. Montazami, N. Hashemi. Viability of Neural Cells on 3D Printed Graphene Bioelectronics. *Biosensors*. 2019, **9**, 112

29. T. Abu- Rahmeh, O. Badran, A. Al-Alawin, N. Nashat. The effect of water temperature and flow rate on cavitation growth in conduits. Mechanical Engineering Department, Faculty of Engineering Technology, Al-Balqa' Applied University, Amman, Jordan, Paper No. 8. http://www.jeaconf.org/UploadedFiles/Document/64541b01-0a47-437e-b3af-79afd07a828f.pdf

30. M. Li, A. Bussoniere, M. Bronson, Z. Xu, Q. Liu. Study of Venturi tube geometry on the hydrodynamic cavitation for the generation of microbubbles. *Minerals Engineering*. 2019, **132**, 268-274

31. N. Vichare, P. Gogate, A, Pandit. Optimization of Hydrodynamic Cavitation Using a Model Reaction. *Chemical Engineering Technol*ogy. 2000, **23**, 683-690

CHAPTER 3. CONCLUSION & FUTURE WORK

The results presented in this thesis indicate that hydrodynamic cavitation assist in exfoliating graphene in aqueous state. This was done using an inexpensive cavitation model which uses a needle valve. Additionally, an optimized cavitation model using a venturi tube is proposed in this thesis with analytical evidence of the effectiveness of the venturi tube in microbubble propagation. Further analytical evidence is presented in the effects of flow rate and temperature in optimizing cavitation at the venturi tube. Despite the promising results found using the cavitation model using the needle valve, a major drawback in this setup was that a centrifugal pump was used instead of a positive displacement pump, for in centrifugal pumps, flow tends to vary with pressure. In an optimized cavitation model, it is crucial that a constant flow is been supplied.

Due to these factors for future experimentation it is recommended that while implementing the proposed venturi tube for the cavitation model a positive displacement pump is being used. Also, as the system pressure is not significantly high it is safe to assume the usage of PVC piping in designing the system should suffice in meeting the pressure requirements. This will help in reducing the production cost of the model.